



# A Facile Preparation of Ambient Pressure–Dried Hydrophilic Silica Aerogels and Their Application in Aqueous Dye Removal

Xianghua Yang<sup>1\*</sup>, Zhixu Wu<sup>1</sup>, Haifeng Chen<sup>1</sup>, Qixuan Du<sup>1</sup>, Lin Yu<sup>1</sup>, Ruiyang Zhang<sup>2</sup> and Ying Zhou<sup>2\*</sup>

<sup>1</sup> Key Laboratory of Clean Chemistry Technology of Guangdong Regular Higher Education Institutions, School of Chemical Engineering and Light Industry, Guangdong University of Technology, Guangzhou, China, <sup>2</sup> State Key Laboratory of Oil and Gas Reservoir Geology and Exploitation, Southwest Petroleum University, Chengdu, China

## OPEN ACCESS

### Edited by:

Hazizan Md. Akil,  
University of Science  
Malaysia, Malaysia

### Reviewed by:

Ann M. Anderson,  
Union College, United States  
Can Erkey,  
Koç University, Turkey  
Wenbo Wang,  
Lanzhou Institute of Chemical Physics  
(CAS), China

### \*Correspondence:

Xianghua Yang  
yangxianghua@gdut.edu.cn  
Ying Zhou  
yzhou@swpu.edu.cn

### Specialty section:

This article was submitted to  
Polymeric and Composite Materials,  
a section of the journal  
Frontiers in Materials

Received: 16 October 2019

Accepted: 29 April 2020

Published: 10 June 2020

### Citation:

Yang X, Wu Z, Chen H, Du Q, Yu L,  
Zhang R and Zhou Y (2020) A Facile  
Preparation of Ambient  
Pressure–Dried Hydrophilic Silica  
Aerogels and Their Application in  
Aqueous Dye Removal.  
Front. Mater. 7:152.  
doi: 10.3389/fmats.2020.00152

Highly porous hydrophilic silica aerogels (SAs) are potentially excellent adsorbents in aqueous media, which are generally synthesized via a standard sol–gel method followed by the relatively complex and specialized high pressure–requiring supercritical fluid drying process. Herein, a facile and novel synthetic method applying ambient pressure–drying technology for the rapid preparation of hydrophilic SAs is reported, and they are simply soaked with metal cation solutions without the need of traditional surface modification or supercritical fluid drying process. Chemical and physical properties of the hydrophilic SAs were characterized and compared with a trimethylchlorosilane (TMCS)-modified hydrophobic silica aerogel. In addition to the integrity and low shrinkage of the as-prepared products, Fourier transform infrared (FTIR) spectra and integrated thermal analyzer (ITA) results revealed the presence of hydroxyl groups as well as the absence of multitudinous hydrophobic groups on the silica surface after soaking. Field emission scanning electron microscope (FE-SEM) and Brunauer–Emmett–Teller (BET) measurements confirmed the mesopores inside the aerogel skeleton. Among the tested metal cations, the Mg<sup>2+</sup>-soaked SAs demonstrated the best pore properties (pore diameter 9.35 nm and pore volume 1.09 cc/g), and the Fe<sup>3+</sup>-soaked ones got the biggest surface area (855.62 m<sup>2</sup>/g) in contrast to other metal cations. Rhodamine B and Methylene blue solutions are used to check the absorption ability of the SAs in aqueous media, in which the best adsorption capacity for Rhodamine B and Methylene blue reached 2.8 and 40.4 mg/g, respectively, implying their potential application in aqueous pollutant removal.

**Keywords:** hydrophilic silica aerogel, metal cations, ambient pressure drying, mesopores material, aqueous dye removal

## INTRODUCTION

Organic dyes, which are widely used in the textile, paper, and cosmetics industries, have been considered as one of the major pollutants in wastewater (Cheng et al., 2014; Yu et al., 2015). To remove the organic dye pollutants from water, physical absorption is a potentially efficient and economical method (Santhy and Selvapathy, 2006; Dawood and Sen, 2012). Recently, silica aerogels

(SAs) with extraordinary physical properties, such as extremely light weight (Bag et al., 2009; Wu et al., 2018), low thermal conductivity (Ryan et al., 2000; Wa et al., 2015; Yang et al., 2015; Zhao et al., 2015; Liu et al., 2017), large specific surface areas, and high porosity (Kota et al., 2014; Yang et al., 2017; Feng et al., 2018), have become well-known as excellent adsorption materials. The large surface area and high porosity can make dye molecules quickly transfer to the surface of SAs, thus accelerating the adsorption process. Additionally, their performance can be easily altered through modification of different functional groups or doping of various catalysts. For example, Liu et al. (2016) obtained a photocatalytic SiO<sub>2</sub> aerogel by modifying WxTiO<sub>2</sub> nanocomposite nanoparticles for the removal of RhB from water. Štandeker et al. (2011) prepared novel SAs with mercaptan functional groups through supercritical drying with CO<sub>2</sub>, which exhibited excellent adsorption ability toward Cu (II) and Hg (II). Han et al. (2016) compared the adsorption capacity of hydrophobic and hydrophilic SAs toward organic dyes. However, SAs are rarely used in aqueous pollutant removal owing to the limitations of the energy-consuming and costly supercritical drying technology (Sarawade et al., 2007; Pierre and Rigacci, 2011; Zhou et al., 2018).

Recently, great efforts have been made to exploit the relatively versatile and economical ambient pressure-drying (APD) technology (Rao et al., 2007; Kim et al., 2008; Hu et al., 2016; Gunay et al., 2018). The employment of organosilane reagent can significantly avoid shrinkage and destruction of the monolithic structure of SAs caused by capillary force during the APD process (Wang et al., 2014; Gunay et al., 2018). However, owing to this hydrophobic modification process, APD-obtained SAs are exclusively hydrophobic, which makes them unsuitable for aqueous applications, such as dye removal (Soleimani Dorcheh and Abbasi, 2008; Shao et al., 2013). Moreover, this modification process is not only time-consuming, but the organosilane reagents are also costly and may lead to a secondary pollution (Jeong et al., 2000; Yin et al., 2017). Therefore, it is still a great challenge to develop an economical and eco-friendly procedure for the manufacturing of hydrophilic SAs (Huang Y. D. et al., 2016; Maleki and Hüsing, 2018).

Herein, we report a facile surface hydroxyl modification method for the synthesis of hydrophilic silica aerogel monoliths by simply applying metal cations as the soak solutions followed by a modified APD technology. This method could not only exempt the utilization of organosilane reagents as well as the hydrophobic modification course, but also shorten the modifying time from 2 days to 1 day. Moreover, the hydrophilicity and porosity of the as-prepared SAs were utilized to absorb organic dyes from aqueous media. The adsorption capacity of the metal cation-modified SAs makes them potential absorbents for aqueous environmental treatment.

## EXPERIMENT

### Materials and Chemicals

Tetraethoxysilane (TEOS), n-hexane ( $\geq 97.0\%$ ) and N, N-dimethylformamide (DMF) ( $\geq 99.5\%$ ) were purchased from Tianjin Damao Chemical Reagent Company, China.

Ethanol (EtOH,  $\geq 99.7\%$ ), ammonia (NH<sub>3</sub>·H<sub>2</sub>O, 25%) came from Guangdong Guanghua Sci-Tech Co. Ltd. and trimethylchlorosilane (TMCS,  $\geq 99.7\%$ ) from Macklin Reagent (Shanghai). Ferric chloride was supplied by Guangzhou Panyu Liqiang Chemical Reagent Company, China; calcium chloride by Guangzhou Chemical Reagent Company, China; barium chloride, magnesium chloride, and copper chloride by Fuchen Chemical Reagent Company, China; and hydrogen chloride by China Sinpharm Chemical Reagent Company. All chemicals were AR grade and used without further purification unless noted.

### Synthesis of Metal Cation Impregnated SiO<sub>2</sub> Aerogels

In a typical two-step sol-gel process, the silica wet gels were generated from TEOS, deionized water, EtOH, and DMF (Rao et al., 1999). The precursor and solvents were charged into a 250 mL round-bottom flask under constantly stirring at a fixed molar ratio of TEOS:EtOH:H<sub>2</sub>O:Hydrochloric acid (0.1 mol/L):DMF equal to 1.5:3:1.6  $\times 10^{-3}$ :0.75. The mixture was stirred for 1 h at 65°C, cooled down to room temperature, and then transferred into a 250 mL beaker, where 1.3 mL NH<sub>3</sub>·H<sub>2</sub>O (0.5 M) was slowly added into the sol while stirring. After being stirred for another 3 min, the agitator was switched off to prevent turbulence and the beaker covered to let the wet gel form steadily at room temperature within 15 min. After aging in EtOH twice in 24 h, the silica gel was soaked in 0.03 mol/L metal salt solutions at the same temperature for 1 day. Afterward, the loaded wet gels were immersed in n-hexane four times in 12 h to exclude water inside the pores. Subsequently, the as-prepared gel was gradually dried at room temperature for 1 day, 60°C for 4 h, and 100°C for 2 h to avoid temperature shock and shrinkage. In order to compare the N<sub>2</sub> adsorption performance of the hybrid aerogels with conventional hydrophobic SiO<sub>2</sub> aerogel, a TMCS-modified silica aerogel was also prepared via a similar sol-gel procedure and APD process. Silica aerogels soaked with different metal ions or modifiers were marked as S1 (Ni<sup>2+</sup>), S2 (Ba<sup>2+</sup>), S3 (Cu<sup>2+</sup>), S4 (Fe<sup>3+</sup>), S5 (Ca<sup>2+</sup>), S6 (Mg<sup>2+</sup>), and S7 (TMCS), respectively.

### Characterization

All the samples were dried at 100°C for at least 5 h before doing BET, TG, and SEM tests, which were performed at room temperature unless otherwise specified. The volume shrinkage of samples was calculated by comparing the change between the volumes of the wet gel and the aerogel. Composite aerogels were ground into subtle powder with KBr and pressed into disks to study their chemical bond information using Fourier transform infrared spectroscopy (FTIR) (Nicolet6700, Thermofisher, USA). Oxidation of the organic groups (-CH<sub>3</sub>) on the silica surface was characterized by means of thermogravimetric analyses (TGA) (STA 409 PC, NETZSCH, Germany) with a heating rate of 10°C/min under an air flow from 25°C up to 800°C. The values of their specific surface area, pore volume, N<sub>2</sub> gas adsorption-desorption isotherm, and pore size distribution of the hydrophobic and hydrophilic SAs were determined by a Brunauer-Emmett-Teller (BET) N<sub>2</sub> gas adsorption/desorption apparatus (TriStar II plus, Micromeritics, USA) via weighing

about 100 mg of powder at 77 K in liquid nitrogen. The pore size distribution originated from the desorption branch of the nitrogen adsorption isotherm by using the Barrett–Joyner–Halenda (BJH) model with a total test time of 24 h. Before the BET and BJH measurement, the as-prepared aerogels were pretreated at 100°C for 6 h under vacuum. The microstructures of the SAs were investigated using a field emission scanning electron microscope (FE-SEM, SU8010, Hitachi). Mg mapping of the fracture surface of the sample was employed to investigate distribution of magnesium on the silica phase throughout the structure.

## Adsorption Activity Test

Methylene blue (MB) was used for evaluating the adsorption capability of metal ion/SiO<sub>2</sub> composite aerogels. First, 0.12 g SAs (ground for 20 min in a mortar) were added into 100 ml MB solution (40 mg/L). During the adsorption experiment, the MB solution was stirred in a dark chamber for an hour at room temperature. The upper clear supernatant liquid was taken after a centrifugal separation process at certain intervals. Then the optical absorbance of the obtained clear liquid was characterized by UV–Vis spectrophotometer (UV759 GD) at wavelength 554 nm for RhB and 664 nm for MB. Finally, the concentration of MB solution varied following adsorption time, which can be determined according to the standard relationship curve between the absorbance and concentration of standard MB solution. The procedure for Rhodamine B (RhB) absorption was exactly the same as for MB.

The adsorption stability of the composite was studied by reusing the same composite material in eight batches of the adsorption experiments. In all eight batches, 100 ml of an aqueous dye (40 mg/L) solution was mixed with 0.12 g of the aerogel and stirred in a dark chamber for an hour at room temperature. The SAs used in the first experiment were subsequently removed from the solution by centrifugation and washed with methanol and deionized water. The washed aerogel was then dried and reused in the second batch of adsorption experiments and so on.

In order to discuss the controlling mechanism of the adsorption process, different kinetic models, i.e., pseudo-first-order, pseudo-second-order, and intra-particle diffusion models, were used to evaluate the experimental data. The linear forms of these three models can be, respectively, expressed as

$$\ln(q_e - q_t) = \ln q_e - k_1 t \quad (1)$$

$$\frac{t}{q_t} = \frac{1}{k_2 q_e^2} + \frac{t}{q_e} \quad (2)$$

$$q_t = k_{id} t_{0.5} \quad (3)$$

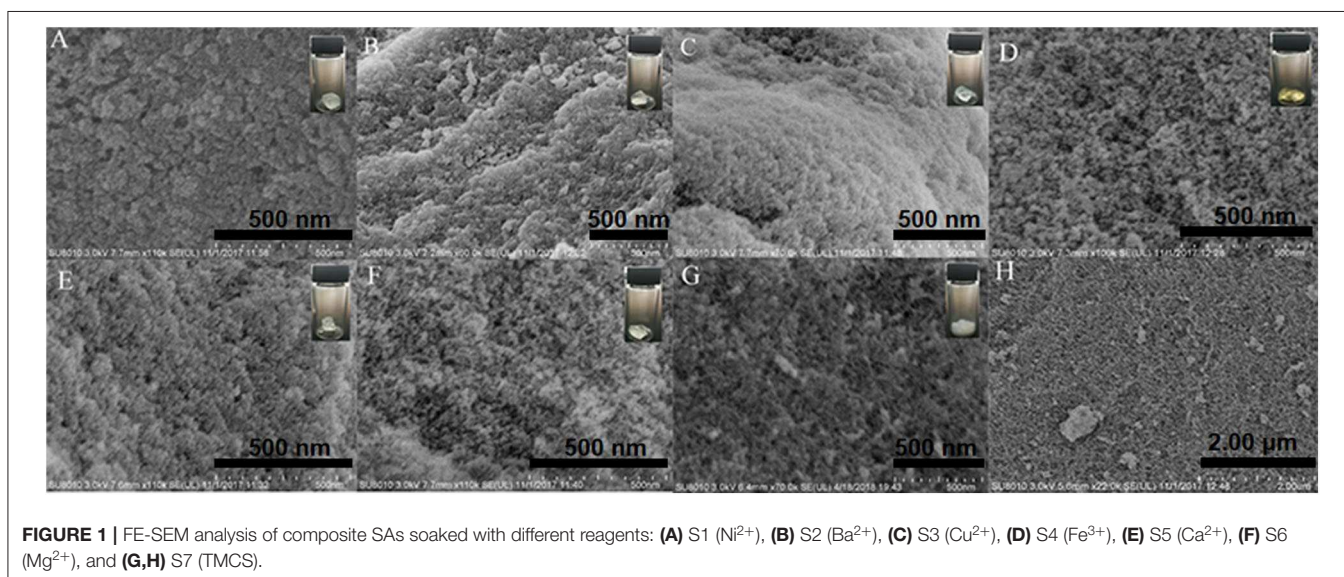
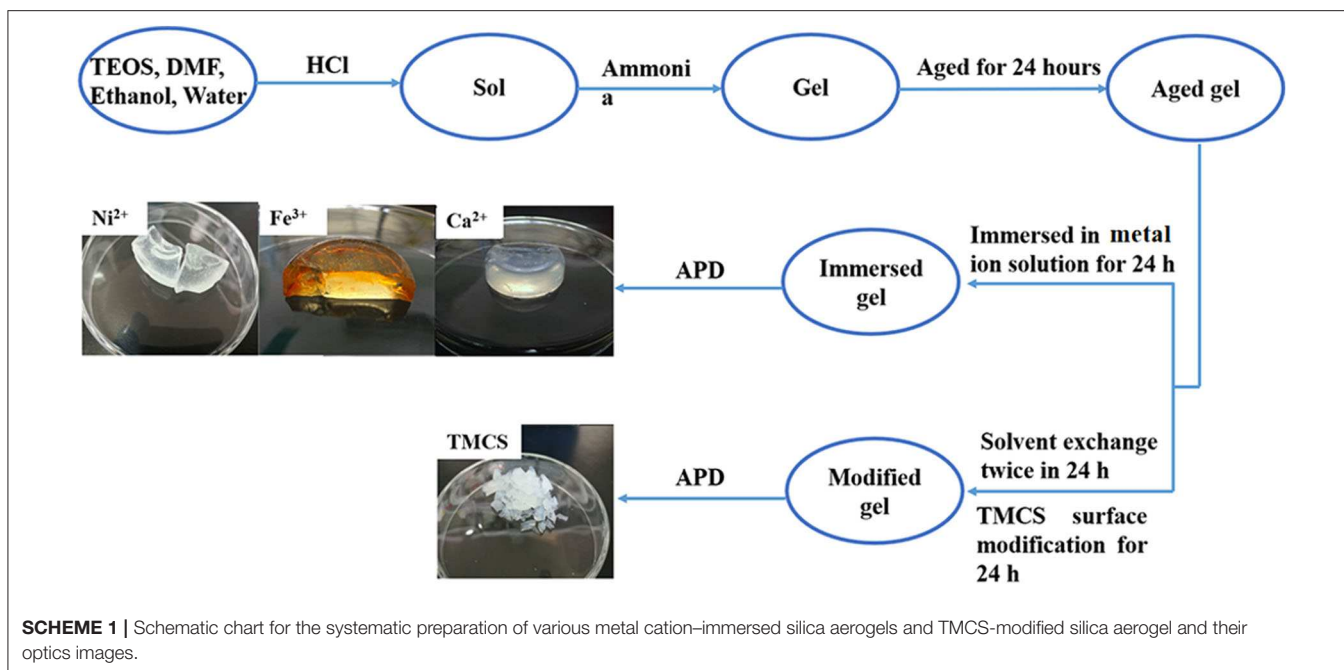
where  $q_e$  and  $q_t$  are the amount of RhB or MB adsorbed on SA powders (mg g<sup>-1</sup>) at equilibrium and at time  $t$ , respectively, and  $k_1$  (min<sup>-1</sup>),  $k_2$  (g·mg<sup>-1</sup> min<sup>-1</sup>), and  $k_{id}$  (mg g<sup>-1</sup> min<sup>-0.5</sup>) are the adsorption rate constant of first-order adsorption, second-order adsorption, and intra-particle diffusion models, respectively. The theoretical values of the adsorption capacity were calculated from the slopes and intercepts of the plots of  $\ln(q_e - q_t)$  vs.  $t$ ,  $t/q_t$  vs.  $t$ , and  $q_t$  vs.  $t_{0.5}$  (Huang X. et al., 2016).

## RESULTS AND DISCUSSION

The synthesis routes of different metal cation-soaked SAs and TMCS-modified SA are shown in **Scheme 1**. It can be clearly seen that, besides the similar sol–gel process, the most significant difference lies in the treatment of the aged gels. For the TMCS-modified SA, 24 h is needed for the solvent exchange and another 24 h for the surface modification, and the metal cation-soaked SAs only need 24 h altogether, which significantly decreases the preparation time. It can be clearly seen that the metal cation-soaked SAs show favorable monolithic properties with low shrinkage after the APD process, which allows them be easily recovered from aqueous solution. In the meantime, the integrity of the TMCS-modified SA is destroyed, resulting in pieces of aerogels several centimeters in diameter.

The micro-structures of the composite aerogels were confirmed by field emission scanning electron microscopy (FE-SEM). Usually, the mesopores in the SAs are damaged to a certain degree because of the surface tension-caused shrinkage if no hydrophobic modification is applied before the APD procedure. As shown in **Figure 1**, all the samples exhibited porous structures, which are consistent with structures of nano-scale SiO<sub>2</sub> particles, resulting in sponge-like FE-SEM micrographs. The differences in micro-morphologies among the composite SAs could possibly be ascribed to diverse formation mechanisms of the nanoporous networks affected by different metal ions, just like the surface hydrophobic modification effect of TMCS. Moreover, this morphology is consistent with that of a typical mesoporous silica aerogel with highly porous structures. Such a morphology implies a metal ion-induced reinforcement of the three-dimensional framework, which is in good accordance with the BET analysis demonstrated later.

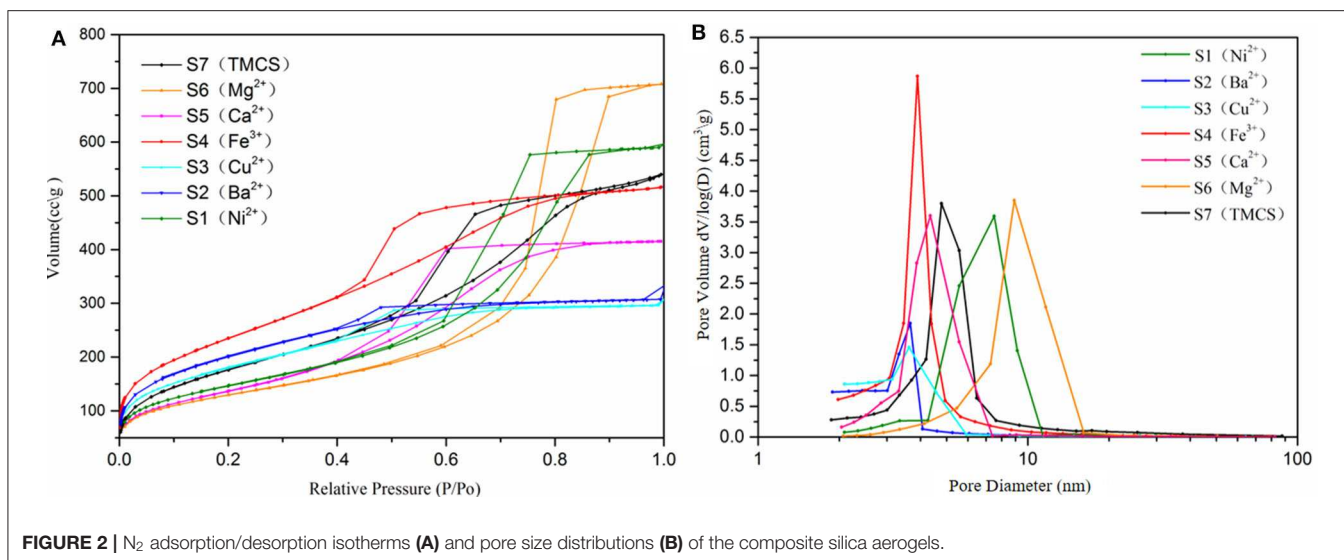
The porosities of the SAs were investigated by nitrogen adsorption–desorption isotherms (**Figure 2A**). Because the shape of a hysteresis loop was usually determined by the pore properties, a lot of information about the pore character can be explored from the isotherms. The isotherms of samples S2 (Ba<sup>2+</sup>) and S3 (Cu<sup>2+</sup>) exhibit a typical adsorption/desorption curve of microporous materials according to their narrow hysteresis loops, which are most probably due to collapses and shrinkages in the frameworks, implying that the SAs obtained with Cu<sup>2+</sup> or Ba<sup>2+</sup> do not have significant enhancement effect (Hwang et al., 2008). The physisorption isotherms of samples S1 (Ni<sup>2+</sup>) and S6 (Mg<sup>2+</sup>) are Type IV, which is one of the most significant characteristics of mesoporous materials, and are similar to aerogels prepared via supercritical drying technology (Hou et al., 2018). For S1 (Ni<sup>2+</sup>) and S6 (Mg<sup>2+</sup>), the first inflection point appeared at a relative pressure of 0.50 while the adsorption reached saturation at around 0.95, indicating a relatively uniform and narrow pore size distribution with tubular cylinder opening at both ends because of the capillary condensation in the SAs according to literature (Pierre and Rigacci, 2011). As for samples S4 (Fe<sup>3+</sup>), S5 (Ca<sup>2+</sup>), and S7 (TMCS), the first inflection point emerged at about 0.85. The large hysteresis loops shown for samples S4 (Fe<sup>3+</sup>), S5 (Ca<sup>2+</sup>), and S7 (TMCS) tally with an H1 type, which represents the existence of an ink-bottle shape in the cross-linked skeleton, indicating that the cations Fe<sup>3+</sup> and



Ca<sup>2+</sup> might have a similar enhancement to the gel skeletons as TMCS. This is most probably due to their interactions with the adjacent -OH groups on the gel surface, leading to a decrease of surface tension during the drying process. The results imply that the existence of Fe (III), Mg (II), Ca (II), and Ni (II) in the gel framework has a significant enhancement on the pore structure of the resulting aerogels during APD.

The specific surface areas, pore volumes, and average pore diameters of the SAs were derived from BET measurements as listed in **Table 1**. The difference in specific surface areas among these SAs is possibly due to the roughness of the surface as seen from SEM. The specific surface areas of the SAs all ranged

between 400 and 900 m<sup>2</sup>/g, where the Fe<sup>3+</sup>-modified sample S4 displayed the highest specific surface area (~855 m<sup>2</sup>/g), and the sample soaked with Mg<sup>2+</sup>, S6, got the largest pore volume comparing to others. The pore size distributions (PSDs) of the composite aerogels were analyzed on the basis of the absorption branches of the isotherms as illustrated in **Figure 2B**. For all the samples S1–S7 narrow PSDs with peaks of pore diameter between 3.5 and 10 nm were discovered, indicating that the mesopores remained after the APD process. Among them, S4 (Fe<sup>3+</sup>) has the narrowest and most uniform pore size distribution while samples S2 (Ba<sup>2+</sup>) and S3 (Cu<sup>2+</sup>) displayed particularly low cumulative pore volumes and irregular PSDs with an unnoticeable pore



diameter peak of 3.5 nm compared to other samples, most probably due to shrinkage of the framework. In addition, the PSDs of samples S1 ( $Ni^{2+}$ ) and S6 ( $Mg^{2+}$ ) are wider than others. For the TMCS-modified sample S7, moderate pore size distribution with a peak of diameter at 4.5 nm was obtained. These results demonstrate that the pore size distribution of the SAs could be tuned by changing of the metal cation.

The chemical bonding information of the SAs modified by different types of metal salts and TMCS were studied using FTIR spectra as shown in **Figure 3A**. The strong absorption peaks at 3,480 and 1,610  $cm^{-1}$  in spectra of S1–S6 correspond to hydroxyl (-OH) stretching vibration, demonstrating that these composite aerogels absorb water in the air and exhibit strong hydrophilicity while the hydrophobic sample S7 (TMCS) only showed weak absorption peaks of Si-OH at  $\sim 980$   $cm^{-1}$  (Al-Oweini and El-Rassy, 2009; Hilonga et al., 2009). The strong absorption peaks of Si-O-Si bonds appeared at around 492 and 1,100  $cm^{-1}$  in all these spectra belonging to the silica network, indicating that TEOS hydrolyzed successfully and formed cross-links, which are typical features of SAs. For sample S7 (TMCS), an absorption peak at 2,990  $cm^{-1}$  associated with the terminal  $-CH_3$  group and vibration peaks of Si-C at 1,280, 840, and 766  $cm^{-1}$  were observed, rooting from surface modification with TMCS (Bhagat et al., 2007). The absence of  $-CH_3$  groups in the IR spectra of samples S1–S6 further proved that they were dried without any methyl modification (Bangsi et al., 2009). As shown in **Figure 1**, the composite aerogel prepared with TMCS exhibited good hydrophobicity and light weight, which could float on water while the aerogel treated with  $Mg^{2+}$  submerged into water quickly owing to its hydrophilicity.

Thermogravimetry analysis (TGA) was performed from 30 to 800°C to study the thermal stabilities of selected samples. The majority of weight loss for composite SAs soaked with different metal ions was observed before 200°C as depicted in **Figure 3B**, revealing that water or residual organic solvents are being removed following elevated temperature in the

framework. Although these samples were dried in an oven for a period of time, the SAs also demonstrated a strong water absorption property according to weight loss of 30% before 200°C. Additionally, no evident weight loss of over 8% was observed after 200°C, representing the absence of organic groups' decomposition, which is consistent with their hydrophilicity as proved by FTIR. Meanwhile, the side product—ammonium chloride ( $NH_4Cl$ )—contained in the sample disappeared because of pyrolysis between 100 and 300°C, which would contribute to partial weight loss of the aerogels (Pan et al., 2017). Because of the difference in binding ability between aerogels and metal ions, the results of weight loss display disparity possibly due to conversion of different content of various metal ions to metal oxides at higher temperatures. Quite on the contrary, sample S7 (TMCS) only showed a negligible weight loss (only about 3%) at temperatures below 250°C but dramatic weight loss of more than 10% was detected after temperature reached 300°C, which could be assigned to the oxidation of organic groups ( $-CH_3$ ) attached on the silica surface (Cheng et al., 2017). The curve gradually tends to be steady when the temperature is higher than 500°C, indicating that the decomposition of  $-CH_3$  basically completed. In general, the weight loss of sample S7 (TMCS) between 30 and 800°C is lower than the other samples. Thus, the SAs with metal ion content had more hydroxyl functional groups than TMCS-modified SA, showing strong hydrophilic properties, which can be according to FTIR analysis.

To further understand the distribution of metal ions inside the aerogel frameworks, the  $Mg^{2+}$ -soaked aerogel with the largest pore volume and biggest pore diameter of all the samples was chosen to undergo Mg mapping analysis, in which the metal ion was found to be evenly distributed on the aerogel right after the APD procedure (**Figure 4A**). The Mg mapping still looks good even after the sample was immersed in water for a whole day (**Figure 4B**), indicating that the metal ions were strongly adhered to the silica network. Based on this, a tentative ion coordination with the composite aerogel was proposed using Cinema 4D as in

**TABLE 1** | Pore properties of TEOS-originated ambient pressure-dried SAs soaked with various reagents.

Sample	Soaking reagent	Volume shrinkage (%)	Pore diameter (nm)	Surface area (m <sup>2</sup> /g)	Pore volume (cc/g)
S1	Ni <sup>2+</sup>	15.2	6.88	530.81	0.91
S2	Ba <sup>2+</sup>	25.6	2.86	713.65	0.52
S3	Cu <sup>2+</sup>	29.5	2.90	652.83	0.47
S4	Fe <sup>3+</sup>	25.5	3.70	855.62	0.80
S5	Ca <sup>2+</sup>	18.4	5.09	504.78	0.64
S6	Mg <sup>2+</sup>	16.7	9.35	468.18	1.09
S7	TMCS	19.6	4.87	650.44	0.84

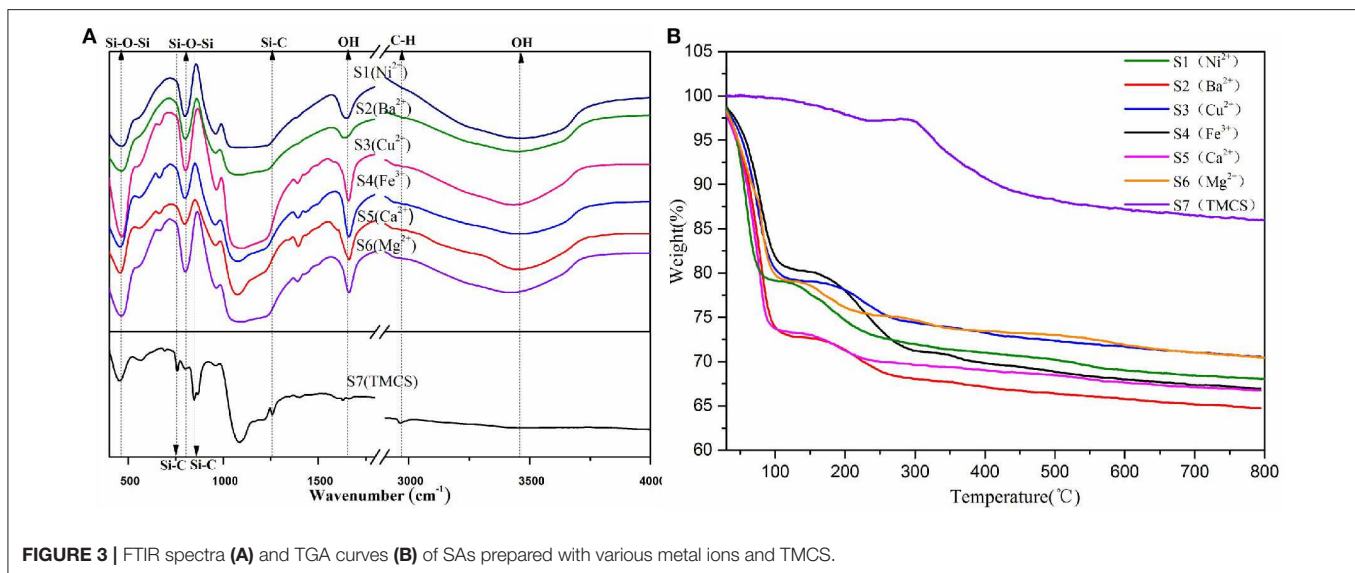
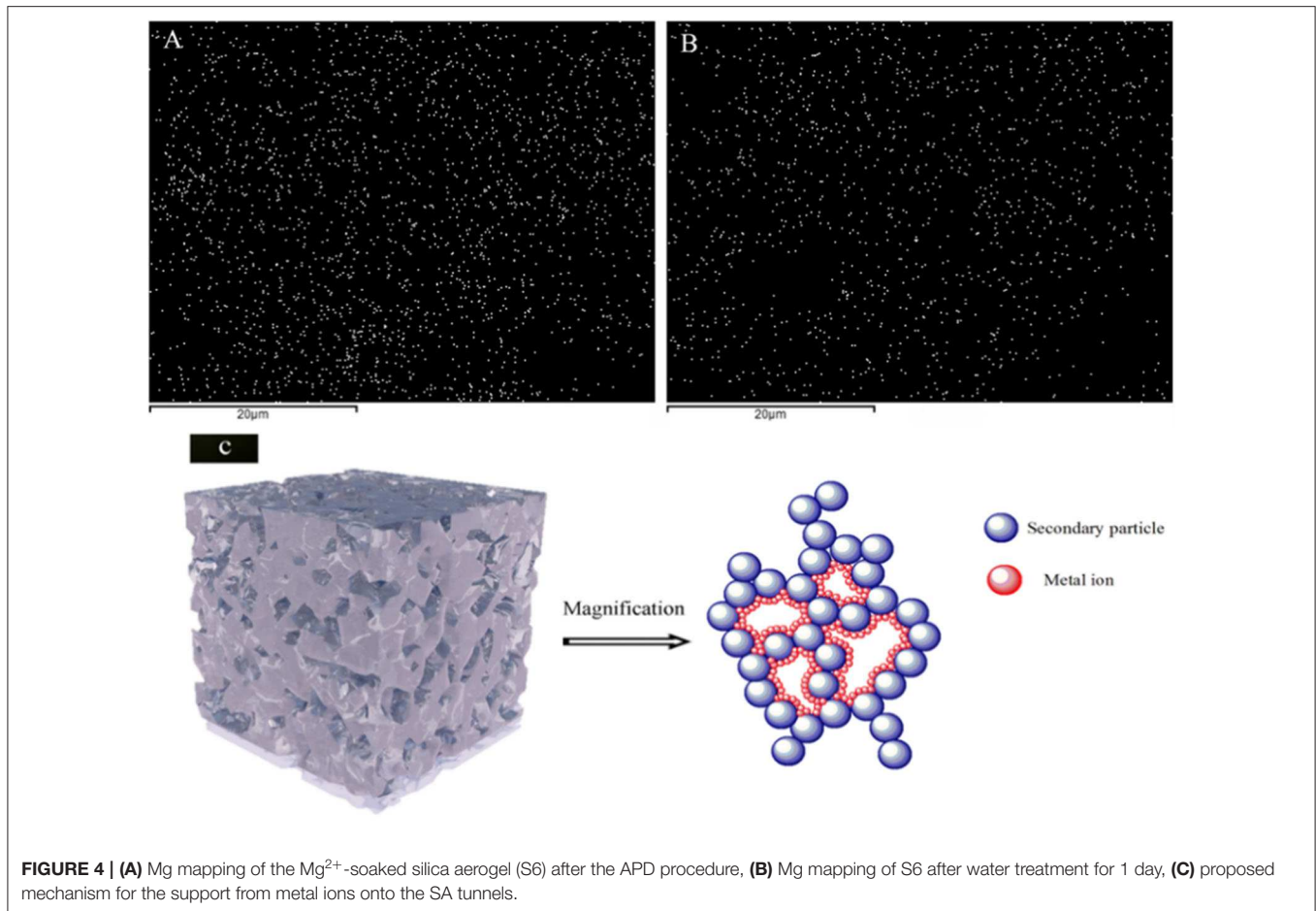


**Figure 4C.** During the soaking phase, the metal ions participate in the connection between the Si-OH groups and the water molecules, which would combine with the hydroxyl groups on the inner wall of the silica tunnel, forming a protective layer to reduce surface tension during the APD stage. Following this hypothesis, other metal ions might also bind to the silica aerogel skeletons through a similar coordinated network. Moreover, the strong water absorption performance represents existence of abundant Si-OH groups on its surface. This result reflected that metal ion has a supporting effect on the SAs skeleton.

Finally, MB and RhB solutions are utilized to test the adsorption capacities of these SAs. **Figures 5A,B** shows the adsorption capacity of sample S6 (Mg<sup>2+</sup>) and the comparison between S6 (Mg<sup>2+</sup>) and S7 (TMCS) for different dyes. In contrast with S6 (Mg<sup>2+</sup>), the amount of MB and RhB in solution decreased inconspicuously as the sample S7 (TMCS), mainly due to the obstruction from hydrophobic groups of aerogels. As shown in **Table S1**, all the metal ion-modified SAs exhibited much better absorbability than the TMCS-modified sample. Compared to the absorption capacity of different SAs, the samples S2 and S6 showed the better adsorption ability. Obviously, the adsorptive capacities of the aerogels not only depend on their surface properties, such as specific surface

areas and pore volumes or diameters, but are also related to other factors, including the hydrophilicity of the adsorbents and/or interactions between the surface and the adsorbates. For the TMCS-modified sample S7, being hydrophobic already determined its poor performance in an aqueous media. Among the metal ion-modified SAs, all except S3 (Cu<sup>2+</sup>) exhibited nearly equally good absorbability toward MB (between 35 and 40 mg/g), which decreased sharply for the treatment of RhB (1.5–3.0 mg/g). The appearance of sample S3 (Cu<sup>2+</sup>) may be attributed to the competitive adsorption between copper ions and MB ions, affected by fixed total initial concentration of Cu<sup>2+</sup> and MB on the adsorption capacity of each adsorbate interfering with the uptake of another following the decrease of total adsorbate uptake in the same system (Wu et al., 2009). The superior absorbability toward MB could be attributed to the fitness between the aerogel pores and MB molecules. The 3-D network of the aerogel exhibits higher preferential adsorption than that of RhB because of the following reasons: First, the large surface-to-volume ratio of the 3-D composite aerogel might give rise to more potential adsorption sites to adsorb dye molecule. Second, the SAs have a high surface-to-volume ratio, large accessibility, and appropriate size of pores for the MB molecule to adsorb and enter into the porous structure, which results in



the higher preferential absorptivity for MB. Third, the different metal ions on the silica surface, the positive charge of ions, and their different orbital layers have impacts on the formation of pore structure and also affect the adsorption mechanism because of covalent electron pair formation between the adsorbate and adsorbent SAs (Wang et al., 2016). However, the dye adsorption capacity of SAs has less than in previous literature (Han et al., 2016). Because the SAs with negative charge mostly adsorb metal ions with positive charge density by electrostatic effect during the soaking process, the result for the decrease of dye adsorption ability is attributed to a competitive relation between cationic dye and metal ions.

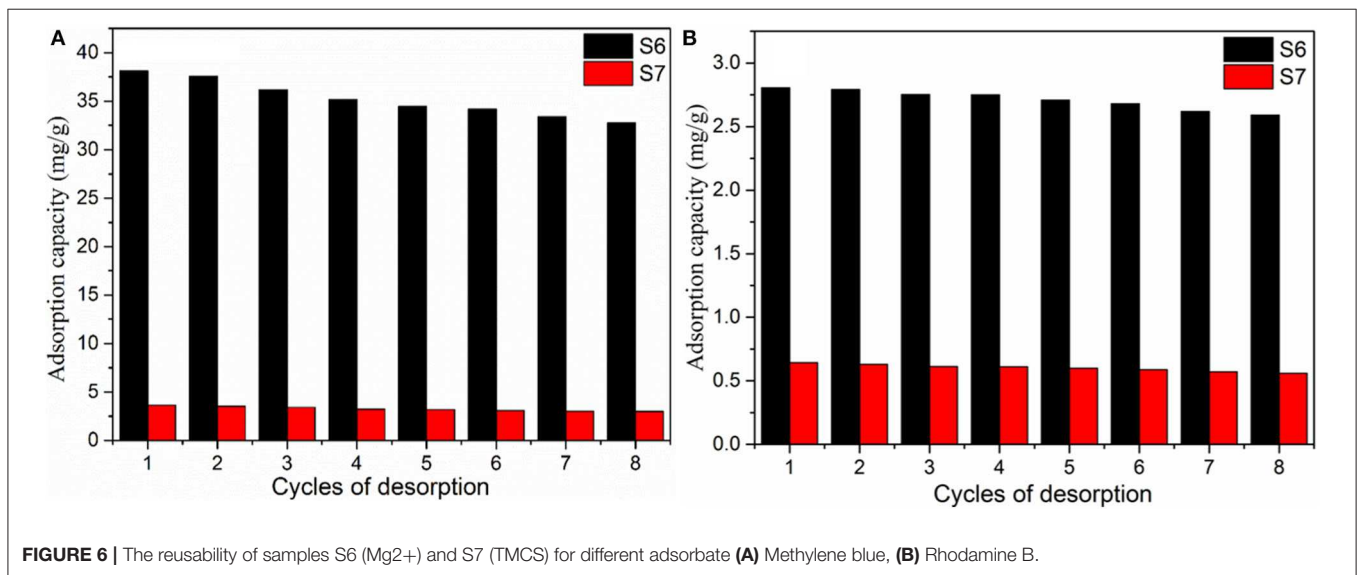
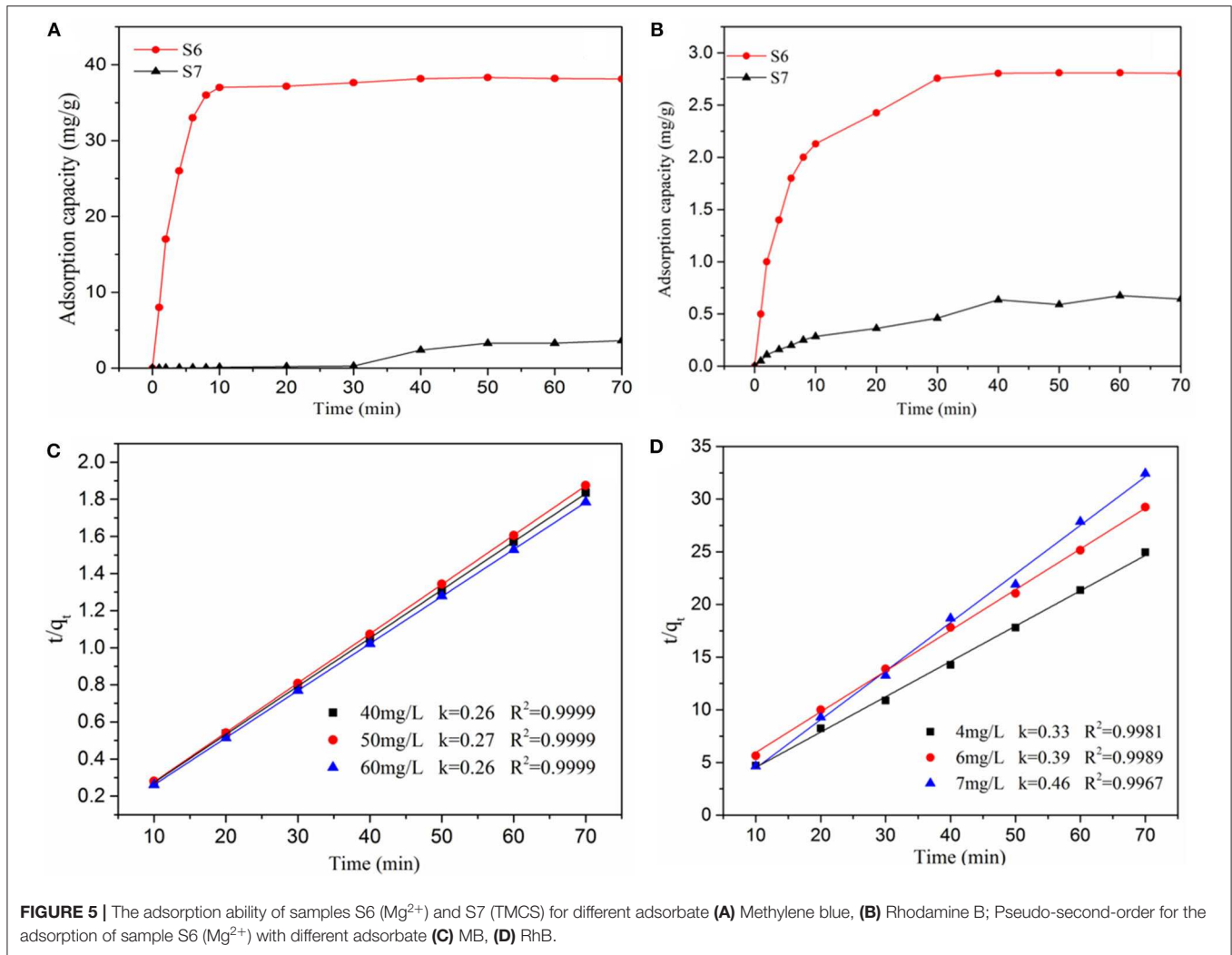
The fitted kinetic parameters of S6 ( $Mg^{2+}$ ) are shown in **Figures 5C,D**, and the related linear regression analysis is shown in the SI. Combined with the fitting parameter R2, the highest correlation coefficient value of the pseudo-second-order model can better describe the kinetic adsorption behavior in the progress.

Due to rigorous ecological and commercial demands for sustainability, repeated reuse of adsorbents is an important parameter for routine applications. In order to significantly reduce the overall cost of adsorption process, an adsorbent should not only have high adsorption capability, but also good desorption properties. From **Figure 6**, it is evident that the

adsorption efficiency of the aerogels is retained even after the eighth cycle of reuse. Reusability of S6 essentially establishes that this material has enough potential for industrial applications.

## CONCLUSIONS

In summary, TEOS-originated hydrophilic SAs were directly prepared via APD process applying various metal ion solutions as the modifying reagents. The as-prepared samples demonstrated excellent hydrophilicity with specific surface areas and pore properties as good as—if not better than—the TMCS-modified hydrophobic aerogels. They were successfully utilized for adsorption of organic dyes in aqueous media. Not surprisingly, lower adsorption ability than average SAs were obtained, probably due to a competition between metal ions and organic dyes inside the porous framework. Besides being potential candidates for aqueous pollutant removal, the existence of abundant -OH groups on the silica pore surface also enables them for various post-modifications, such as adoption of functional groups and/or catalysts, formation of hydrogen bonding, etc. However, the existence state of metal ions in the adsorbent as well as the actual interaction mechanism between the metal ions and the aerogel framework are still under further exploration.



## DATA AVAILABILITY STATEMENT

All datasets generated for this study are included in the article/**Supplementary Material**.

## AUTHOR CONTRIBUTIONS

XY designed the experiment and revised paper. ZW carried out date and drafted the manuscript. QD and HC performed the experiment. LY provided equipment testing. YZ and RZ provided assistance for data acquisition, data analysis, and statistical analysis. All authors read and approved the final manuscript.

## REFERENCES

- Al-Oweini, R., and El-Rassy, H. (2009). Synthesis and characterization by FTIR spectroscopy of silica aerogels prepared using several Si(OR)<sub>4</sub> and R<sup>m</sup>Si(OR)<sub>3</sub> precursors. *J. Mol. Struct.* 919, 140–145. doi: 10.1016/j.molstruc.2008.08.025
- Bag, S., Gaudette, A. F., Bussell, M. E., and Kanatzidis, M. G. (2009). Spongy chalcogels of non-platinum metals act as effective hydrodesulfurization catalysts. *Nat. Chem.* 1:217. doi: 10.1038/nchem.208
- Bangi, U. K. H., Parvathy Rao, A., Hirashima, H., and Venkateswara Rao, A. (2009). Physico-chemical properties of ambiently dried sodium silicate based aerogels catalyzed with various acids. *J. Sol Gel Sci. Technol.* 50, 87–97. doi: 10.1007/s10971-008-1887-9
- Bhagat, S. D., Kim, Y.-H., Ahn, Y.-S., and Yeo, J.-G. (2007). Rapid synthesis of water-glass based aerogels by *in situ* surface modification of the hydrogels. *Appl. Surf. Sci.* 253, 3231–3236. doi: 10.1016/j.apsusc.2006.07.016
- Cheng, S., Liu, X., Yun, S., Luo, H., and Gao, Y. (2014). SiO<sub>2</sub>/TiO<sub>2</sub> composite aerogels: preparation via ambient pressure drying and photocatalytic performance. *Ceram. Int.* 40, 13781–13786. doi: 10.1016/j.ceramint.2014.05.093
- Cheng, X., Li, C., Shi, X., Li, Z., Gong, L., and Zhang, H. (2017). Rapid synthesis of ambient pressure dried monolithic silica aerogels using water as the only solvent. *J. Porous Mater.* 204, 157–160. doi: 10.1016/j.matlet.2017.05.107
- Dawood, S., and Sen, T. K. (2012). Removal of anionic dye Congo red from aqueous solution by raw pine and acid-treated pine cone powder as adsorbent: equilibrium, thermodynamic, kinetics, mechanism and process design. *Water Res.* 46, 1933–1946. doi: 10.1016/j.watres.2012.01.009
- Feng, Q., Chen, K., Ma, D., Lin, H., Liu, Z., Qin, S., et al. (2018). Synthesis of high specific surface area silica aerogel from rice husk ash via ambient pressure drying. *Colloids Surf. A* 539, 399–406. doi: 10.1016/j.colsurfa.2017.12.025
- Gunay, A. A., Kim, H., Nagarajan, N., Lopez, M., Kantharaj, R., Alsaati, A., et al. (2018). Optically transparent thermally insulating silica aerogels for solar thermal insulation. *ACS Appl. Mat. Interfaces* 10, 12603–12611. doi: 10.1021/acsami.7b18856
- Han, H., Wei, W., Jiang, Z., Lu, J., Zhu, J., and Xie, J. (2016). Removal of cationic dyes from aqueous solution by adsorption onto hydrophobic/hydrophilic silica aerogel. *Colloids Surf. A* 509, 539–549. doi: 10.1016/j.colsurfa.2016.09.056
- Hilonga, A., Kim, J.-K., Sarawade, P. B., and Kim, H. T. (2009). Low-density TEOS-based silica aerogels prepared at ambient pressure using isopropanol as the preparative solvent. *J. Alloys Compd.* 487, 744–750. doi: 10.1016/j.jallcom.2009.08.055
- Hou, X., Zhang, R., and Fang, D. (2018). An ultralight silica-modified ZrO<sub>2</sub>-SiO<sub>2</sub> aerogel composite with ultra-low thermal conductivity and enhanced mechanical strength. *Scripta Mater.* 143, 113–116. doi: 10.1016/j.scriptamat.2017.09.028
- Hu, S.-C., Shi, F., Liu, J.-X., Yu, L., and Liu, S.-H. (2016). Magnetic mesoporous iron oxide/silica composite aerogels with high adsorption ability for organic pollutant removal. *J. Porous Mater.* 23, 655–661. doi: 10.1007/s10934-015-0120-9

## FUNDING

We thank the One-Hundred Young Talents start-up R&D funding of Guangdong University of Technology, the Scientific Program of Guangdong Province (2016B020241003), and the Innovative Research Team of Sichuan Province (2016TD0011) for financial support.

## SUPPLEMENTARY MATERIAL

The Supplementary Material for this article can be found online at: <https://www.frontiersin.org/articles/10.3389/fmats.2020.00152/full#supplementary-material>

- Huang, X., Liu, J. X., Shi, F., Yu, L., and Liu, S. H. (2016). Ambient pressure drying synthesis of Cs<sub>0.33</sub>WO<sub>3</sub>/SiO<sub>2</sub> composite aerogels for efficient removal of Rhodamine B from water. *Adv. Powder Technol.* 110, 624–632. doi: 10.1016/j.matdes.2016.08.031
- Huang, Y. D., Gao, X. D., Gu, Z. Y., and Li, X. M. (2016). Amino-terminated SiO<sub>2</sub> aerogel towards highly-effective lead (II) adsorbent via the ambient drying process. *J. Non Cryst. Solids* 443, 39–46. doi: 10.1016/j.euromechsol.2016.06.006
- Hwang, S. W., Kim, T. Y., and Hyun, S. H. (2008). Optimization of instantaneous solvent exchange/surface modification process for ambient synthesis of monolithic silica aerogels. *J. Colloid Interface Sci.* 322, 224–230. doi: 10.1016/j.jcis.2008.02.060
- Jeong, A. Y., Koo, S. M., and Kim, D. P. (2000). Characterization of Hydrophobic SiO<sub>2</sub> Powders Prepared by Surface Modification on Wet Gel. *J. Sol Gel Sci. Technol.* 19, 483–487. doi: 10.1023/A:1008716017567
- Kim, C. E., Yoon, J. S., and Hwang, H. J. (2008). Synthesis of nanoporous silica aerogel by ambient pressure drying. *J. Sol Gel Sci. Technol.* 49, 47–52. doi: 10.1007/s10971-008-1828-7
- Kota, A. K., Kwon, G., and Tuteja, A. (2014). The design and applications of superomniphobic surfaces. *NPG Asia Mater.* 6:e109. doi: 10.1038/am.2014.34
- Liu, H., Xia, X., Xie, X., Ai, Q., and Li, D. (2017). Experiment and identification of thermal conductivity and extinction coefficient of silica aerogel composite. *Int. J. Therm. Sci.* 121, 192–203. doi: 10.1016/j.ijthermalsci.2017.07.014
- Liu, J., Wang, X., Shi, F., Yu, L., Liu, S., Hu, S., et al. (2016). Synthesis of mesoporous SiO<sub>2</sub> aerogel/Wx TiO<sub>2</sub> nanocomposites with high absorptivity and photocatalytic activity. *Adv. Powder Technol.* 27, 1781–1789. doi: 10.1016/j.apt.2016.06.009
- Maleki, H., and Hüsing, N. (2018). Current status, opportunities and challenges in catalytic and photocatalytic applications of aerogels: environmental protection aspects. *Appl. Catal. B Environ.* 221, 530–555. doi: 10.1016/j.apcatb.2017.08.012
- Pan, Y., He, S., Cheng, X., Li, Z., Li, C., Huang, Y., et al. (2017). A fast synthesis of silica aerogel powders-based on water glass via ambient drying. *J. Sol Gel Sci. Technol.* 82, 594–601. doi: 10.1007/s10971-017-4312-4
- Pierre, A. C., and Rigacci, A. (2011). *SiO<sub>2</sub> Aerogels, Aerogels Handbook*. New York, NY: Springer, 21–45.
- Rao, A. P., Rao, A. V., and Pajonk, G. M. (2007). Hydrophobic and physical properties of the ambient pressure dried silica aerogels with sodium silicate precursor using various surface modification agents. *Appl. Surf. Sci.* 253, 6032–6040. doi: 10.1016/j.apsusc.2006.12.117
- Rao, A. V., Sakhare, H. M., Tamhankar, A. K., Shinde, M. L., Gadave, D. B., and Wagh, P. B. (1999). Influence of N, N-dimethylformamide additive on the physical properties of citric acid catalyzed TEOS silica aerogels. *Mater. Chem. Phys.* 60, 268–273. doi: 10.1016/S0254-0584(99)00089-9
- Ryan, J. V., Berry, A. D., Anderson, M. L., Long, J. W., Stroud, R. M., Cepak, V. M., et al. (2000). Electronic connection to the interior of a mesoporous insulator withnanowires of crystalline RuO<sub>2</sub>. *Nature* 406, 169–172. doi: 10.1038/35018040
- Santhy, K., and Selvapathy, P. (2006). Removal of reactive dyes from wastewater by adsorption on coir pith activated carbon. *Bioresour. Technol.* 97, 1329–1336. doi: 10.1016/j.biortech.2005.05.016

- Sarawade, P. B., Kim, J.-K., and Kim, H.-K., and Kim, H.-T. (2007). High specific surface area TEOS-based aerogels with large pore volume prepared at an ambient pressure. *Appl. Surf. Sci.* 254, 574–579. doi: 10.1016/j.apsusc.2007.06.063
- Shao, Z., Luo, F., Cheng, X., and Zhang, Y. (2013). Superhydrophobic sodium silicate based silica aerogel prepared by ambient pressure drying. *Mater. Chem. Phys.* 141, 570–575. doi: 10.1016/j.matchemphys.2013.05.064
- Soleimani Dorcheh, A., and Abbasi, M. H. (2008). Silica aerogel; synthesis, properties and characterization. *J. Mater. Process. Technol.* 199, 10–26. doi: 10.1016/j.jmatprotec.2007.10.060
- Štandeker, S., Veronovski, A., Novak, Z., and Knez, Ž. (2011). Silica aerogels modified with mercapto functional groups used for Cu(II) and Hg(II) removal from aqueous solutions. *Desalination* 269, 223–230. doi: 10.1016/j.desal.2010.10.064
- Wa, L., Fengyun, L., Fanlu, Z., Mengjing, C., Qiang, C., Jue, H., et al. (2015). Preparation of silica aerogels using CTAB/SDS as template and their efficient adsorption. *Appl. Surf.* 353, 1031–1036. doi: 10.1016/j.apsusc.2015.06.204
- Wang, D., Zhang, J., Guo, L., Dong, X., Shen, H., and Fu, F. (2016). Synthesis of nano-porous Bi<sub>2</sub>WO<sub>6</sub> hierarchical microcrystal with selective adsorption for cationic dyes. *Mater. Res. Bull.* 83, 387–395. doi: 10.1016/j.materresbull.2016.06.029
- Wang, J., Wei, Y., He, W., and Zhang, X. (2014). A versatile ambient pressure drying approach to synthesize silica-based composite aerogels. *RSC Adv.* 4, 51146–51155. doi: 10.1039/C4RA10607E
- Wu, X., Fan, M., Shen, X., Cui, S., and Tan, G. (2018). Silica aerogels formed from soluble silicates and methyl trimethoxysilane (MTMS) using CO<sub>2</sub> gas as a gelation agent. *Ceram. Int.* 44, 821–829. doi: 10.1016/j.ceramint.2017.10.005
- Wu, Y., Zhang, L., Gao, C., Ma, J., Ma, X., and Han, R. (2009). Adsorption of copper ions and methylene blue in a single and binary system on wheat straw. *J. Chem. Eng. Data* 54, 3229–3234. doi: 10.1021/je900220q
- Yang, H., Ye, F., Liu, Q., Liu, S., Gao, Y., and Liu, L. (2015). A novel silica aerogel/porous Si<sub>3</sub>N<sub>4</sub> composite prepared by freeze casting and sol-gel impregnation with high-performance thermal insulation and wave-transparent. *Mater. Lett.* 138, 135–138. doi: 10.1016/j.matlet.2014.10.012
- Yang, J., Wu, H., Huang, G., Liang, Y., and Liao, Y. (2017). Modeling and coupling effect evaluation of thermal conductivity of ternary opacifier/fiber/aerogel composites for super-thermal insulation. *Mater. Des.* 133, 224–236. doi: 10.1016/j.matdes.2017.07.056
- Yin, R., Cheng, H., Hong, C., and Zhang, X. (2017). Synthesis and characterization of novel phenolic resin/silicone hybrid aerogel composites with enhanced thermal, mechanical and ablative properties. *Composites Part A* 101, 500–510. doi: 10.1016/j.compositesa.2017.07.012
- Yu, Y., Zhu, M., Liang, W., Rhodes, S., and Fang, J. (2015). Synthesis of silica-titania composite aerogel beads for the removal of Rhodamine B in water. *RSC Adv.* 5, 72437–72443. doi: 10.1039/C5RA13625C
- Zhao, S., Malfait, W. J., Demilecamps, A., Zhang, Y., Brunner, S., Huber, L., et al. (2015). Strong, thermally superinsulating biopolymer-silica aerogel hybrids by cogelation of silicic acid with pectin. *Angew. Chem. Int. Ed.* 54, 14282–14286. doi: 10.1002/anie.201507328
- Zhou, T., Cheng, X., Pan, Y., Li, C., Gong, L., and Zhang, H. (2018). Mechanical performance and thermal stability of glass fiber reinforced silica aerogel composites based on co-precursor method by freeze drying. *Appl. Surf. Sci.* 437, 321–328. doi: 10.1016/j.apsusc.2017.12.146

**Conflict of Interest:** The authors declare that the research was conducted in the absence of any commercial or financial relationships that could be construed as a potential conflict of interest.

Copyright © 2020 Yang, Wu, Chen, Du, Yu, Zhang and Zhou. This is an open-access article distributed under the terms of the Creative Commons Attribution License (CC BY). The use, distribution or reproduction in other forums is permitted, provided the original author(s) and the copyright owner(s) are credited and that the original publication in this journal is cited, in accordance with accepted academic practice. No use, distribution or reproduction is permitted which does not comply with these terms.